KKU Engineering Journal

https://www.tci-thaijo.org/index.php/easr/index

Published by the Faculty of Engineering, Khon Kaen University, Thailand

Low frequency wireless power transfer using modified parallel resonance matching at a complex load

Artit Rittiplang*[1)], Wanchai Pijitrojana[1)] and Komson Daroj[2)]

[1)]Department of Electrical and Computer Engineering, Thammasat University, Thailand
[2)]Department of Electrical Engineering, Ubon Ratchathani University, Thailand

Received April 2016
Accepted May 2016

Abstract

Series resonant and strong coupling structures under an impedance matching (IM) condition of wireless power transfer (WPT) have been widely studied. These operate under an optimal resistive load and high resonant frequency of greater than 1 MHz. However, the optimal parameters (particular values) limit the design. The common loads are complex and the high frequency RF sources used are usually inefficient. This paper presents a modified parallel resonant (PR) structure that can operate at a low frequency of 15 kHz without an optimal parameter under an IM condition with a complex load. The calculated and experimental efficiencies for a 5 cm transfer distance were 71.2 % at 15 kHz and 68% at 17 kHz, respectively. Hence, a modified two-coil PR structure can be operated at a low frequency with high efficiency.

Keywords: Low frequency wireless power transfer, Modified parallel resonance, Impedance matching, Wireless power transfer

1. Introduction

WPT is a transmission mechanism of the electrical power from the power source for electrical loads without using cables and contacts. The first WPT has existed long before the origin of life. It is solar energy, which is used to drive for the food chain, life, etc. Around 1900, Nikola Tesla did the experiment of a WPT by using the Tesla Coils (Electric Coupling). In 1963, William C. Brown demonstrated a WPT by Microwave (Far field). However, in order to achieve the high efficiency the presented mechanisms, they would require the line-of-sight transmission [1]. In recent years, WPT is based on Magnetic Resonant Coupling (MRC) as highlighted in Figure 1 which have been widely used for many applications because the magnetic field weakly interacts with other materials in surrounding [2].

The two-coil Series Resonance (SR) and strong coupling structures are also popular as shown in Figure 2, these structures are easy to be designed by using the resonant frequency ($f_0=1/2\pi\sqrt{LC}$) with an optimal parameter for achieving the IM condition [1-7]. However, there are various problems as described below.

1. Most of the resonant frequency f_0 is set to greater than 1 MHz for obtaining the high efficiency [2-7] as shown in Figure 3 [6]. But the high frequency RF sources are usually inefficient [2].

2. An optimal parameter is a particular value that is commonly found either an optimal transfer distance or an optimal resistive load [1-7], which causes to limit the design.

3. These structures are difficult to be implemented in case of a complex load for achieving the IM condition once the secondary capacitor and coil are fabricated.

For improving the first problem, the Parallel Resonance (PR) structure can operate at a low frequency of less than 20 kHz [1]. Also, the second and third problems can be solved by adding a series inductor (L_C) in the PR structure to be the compensator as shown in Figure 4.

The modified PR structure can operate at a low frequency of 15 kHz with arbitrary parameters under the IM condition. This paper presents the modified PR structure with a step-by-step design process, and proposes an accurate equivalent circuit model (the resistive losses of the coils are not neglected). In addition, the resistive loss is an important factor which determines the efficiency of the WPT. So this mechanism (adding L_C) is selected because its resistive loss is less than the resistive losses of the matching networks (at least two lump-devices).

2. Individual models

To start the designing of a WPT, we have to obtain electrical parameters from the two-coil sizes of Figure 4. The equivalent circuit of Figure 4 can be shown in Figure 5.

The resistances (R_1 and R_2), the mutual inductance (M), the accurate self-inductance (L_1 and L_2), and the secondary capacitor (C_2) are described below.

1. R_1 and R_2 can be calculated from (1) [8].

*Corresponding author.
Email address: artit_200@hotmail.com*; pwanchai@engr.tu.ac.th; daroj@hotmail.com
doi: 10.14456/kkuenj.2016.30

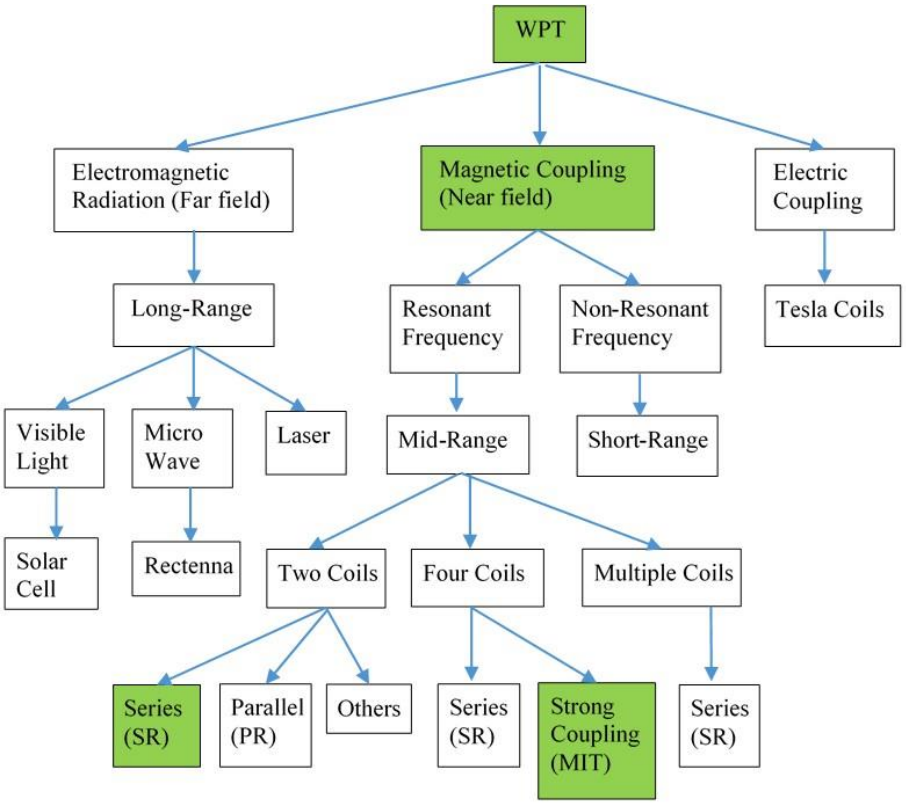

Figure 1 Most of WPT can be mainly categorized into three types [1-9]

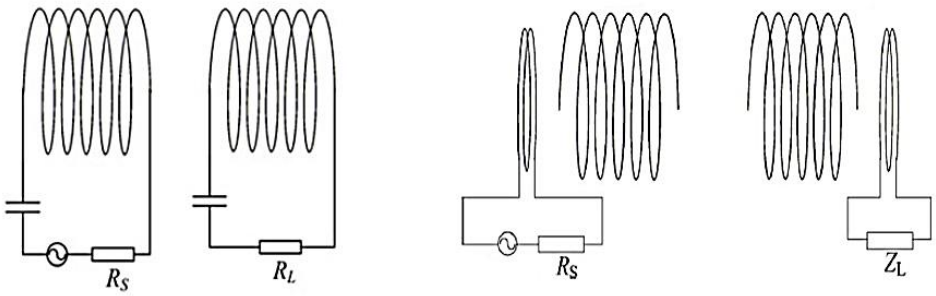

Figure 2 Typical diagram: (a) Two-coil SR structure. (b) Strong Coupling structure, IEEE copyright [5]

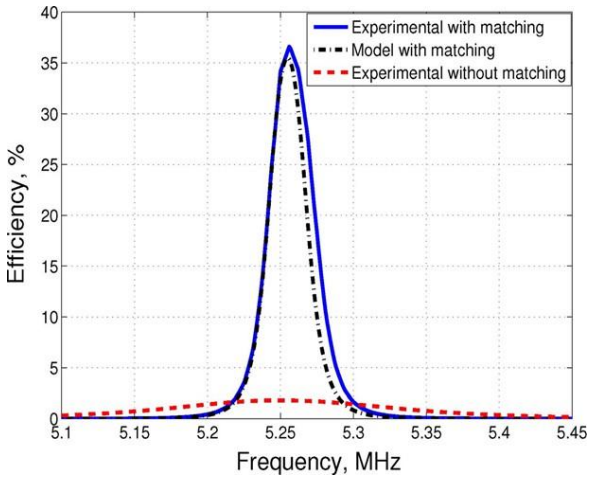

Figure 3 The two-coil SR structure of the ten-turn at the transfer distance of 56 cm shows the high efficiency at about 5.26 MHz, IEEE copyright [6].

$$R = \frac{\rho l}{\pi\delta\left(1 - e^{-\frac{b}{\delta}}\right)\left(2b - \delta\left(1 - e^{-\frac{b}{\delta}}\right)\right)} \quad (1)$$

In which,

$$\delta = \sqrt{\frac{\rho}{\pi\mu_0 f}} \quad (2)$$

$$l = \sqrt{(2a\pi N)^2 + h^2} \quad (3)$$

Where ρ is the resistivity of copper (1.68×10^{-8} Ω. m), μ_0 is the free space permeability constant ($4\pi\times10^{-7}$ H·m^{-1}), l is the length of the conductor, and δ is the skin depth.

2. M can be calculated as shown below [1]

$$M = N_1 N_2 \mu_0 \sqrt{a_1 a_2}\left[\left(\frac{2}{k} - k\right)K(k) - \frac{2}{k}E(k)\right] \quad (4)$$

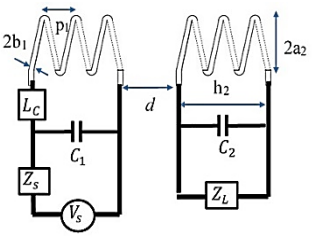

a_1	Primary loop radius	C_1	Primary capacitor
a_2	Secondary loop radius	C_2	Secondary capacitor
b_1	Primary wire radius	Z_L	Complex load ($R_L + jX_L$)
b_2	Secondary wire radius	Z_s	the inner impedance of the RF source
p_1	Pitch of primary coil	V_s	Voltage source
p_2	Pitch of secondary coil	L_C	Compensated inductor
h_1	Height of primary coil	N_1	Number of primary turns
h_2	Height of secondary coil	N_2	Number of secondary turns
d	Transfer distance		

Figure 4 Typical diagram of the modified PR structure

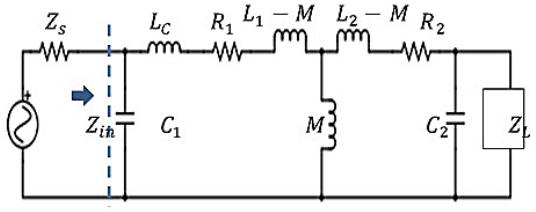

Figure 5 Equivalent circuits of modified PR structure and RF source

where $K(k)$ and $E(k)$ are the first and second kind of elliptic integrations, respectively. They are solved by the numerical integration.

$$K(k) = \int_0^{\frac{\pi}{2}} \frac{d\theta}{\sqrt{1 - k^2 sin^2\theta}} \tag{5}$$

$$E(k) = \int_0^{\frac{\pi}{2}} \sqrt{1 - k^2 sin^2\theta}\, d\theta \tag{6}$$

Where,

$$k = \sqrt{\frac{4a_1a_2}{(a_1 + a_2)^2 + d^2}} \tag{7}$$

3. L_1 and L_2 can be obtained by (8) [7].

$$L = \frac{\mu_0\pi(2a)^2N^2}{4h} k_L - \mu_0 aN(k_s + k_m) \tag{8}$$

Where,

$$k_s = \frac{3}{2} - \ln\left(\frac{p}{b}\right) \tag{9}$$

$$k_m = \ln(2\pi) - \frac{3}{2} - \frac{\ln(N)}{6N} - \frac{0.33084236}{N} - \frac{1}{120N^3} + \frac{1}{504N^5} - \frac{0.0011923}{N^7} + \frac{0.0005068}{N^9} \tag{10}$$

$$k_L = \frac{h}{\pi a}\left[\frac{\left(\ln\left(\frac{8a}{h}\right) - 0.5\right)\left(1 + 0.383901\left(\frac{h}{2a}\right)^2 + 0.017108\left(\frac{h}{2a}\right)^4\right)}{1 + 0.258952\left(\frac{h}{2a}\right)^2} + 0.093842\left(\frac{h}{2a}\right)^2 + 0.002029\left(\frac{h}{2a}\right)^4 - 0.000801\left(\frac{h}{2a}\right)^6\right] \tag{11}$$

4. The secondary capacitance is calculated as shown in (12) to increase the load voltage [8].

$$C_2 = \frac{1}{L_2\omega^2} \tag{12}$$

3. Theory

From Figure 5, the IM condition ($Z_s^* = Z_{in}$) is the maximum power transfer from the RF source to the input impedance Z_{in} [9]. Accordingly, we must calculate L_C and C_1 for achieving the IM condition as shown in (13) and (14), respectively. They are obtained by using L-section matching formulas [9].

$$L_C = \frac{\sqrt{\alpha(Z_s - \alpha)} - \beta}{\omega} \tag{13}$$

$$C_1 = \frac{1}{\omega Z_s}\sqrt{\frac{Z_s - \alpha}{\alpha}} \tag{14}$$

Where,

$$\alpha = R_1 + \frac{\omega^2M^2(R_2 + Y)}{A} \tag{15}$$

$$\beta = \omega L_1 - \frac{\omega^2M^2\left(\omega L_2 - \omega C_2R_LY + \frac{(X_L - \omega C_2X_L^2)Y}{R_L}\right)}{A} \tag{16}$$

$$A = (R_2 + Y)^2 + \left(\omega L_2 - \omega C_2R_LY + \frac{(X_L - \omega C_2X_L^2)Y}{R_L}\right)^2 \tag{17}$$

$$Y = \frac{R_L}{(1 - \omega C_2X_L)^2 + \omega^2C_2^2R_L^2} \tag{18}$$

The input impedance Z_{in} as shown in (19) is calculated to check the IM condition, $Z_s = Z_{in}$?.

$$Z_{in} = \frac{\alpha}{(1 - \omega C_1\beta_c)^2 + \omega^2C_1^2\alpha^2} + j\frac{\beta_c - \omega C_1\beta_c^2 - \omega C_1\alpha^2}{(1 - \omega C_1\beta_c)^2 + \omega^2C_1^2\alpha^2} \tag{19}$$

Where,

$$\beta_c = \omega(L_C + L_1) - \frac{\omega^2M^2\left(\omega L_2 - \omega C_2R_LY + \frac{(X_L - \omega C_2X_L^2)Y}{R_L}\right)}{A} \tag{20}$$

The efficiency (η) of the system can be conveniently calculated by using the Z-and $ABCD$-parameter matrixes as described from (21) - (23) [8].

$$\eta = \frac{Re\{Z_L\}}{Re\{Z_{in}\}}\left|\frac{Z_{21}}{Z_{22} + Z_L}\right|^2 * 100 \tag{21}$$

Where,

$$\begin{bmatrix} Z_{11} & Z_{12} \\ Z_{21} & Z_{22} \end{bmatrix} = \begin{bmatrix} \frac{A_a}{C_c} & \frac{A_aD_d - B_bC_c}{C_c} \\ \frac{1}{C_c} & \frac{D_d}{C_c} \end{bmatrix} \tag{22}$$

$$\begin{bmatrix} A_a & B_b \\ C_c & D_d \end{bmatrix} = \begin{bmatrix} 1 & 0 \\ j\omega C_1 & 1 \end{bmatrix} \begin{bmatrix} 1 & R_1 + j\omega(L_C + L_1) \\ 0 & 1 \end{bmatrix} \begin{bmatrix} 0 & -j\omega M \\ \frac{-j}{\omega M} & 0 \end{bmatrix} \cdots \begin{bmatrix} 1 & R_2 + j\omega L_2 \\ 0 & 1 \end{bmatrix} \begin{bmatrix} 1 & 0 \\ j\omega C_2 & 1 \end{bmatrix} \quad (23)$$

Consequently, we describe the design process of the proposed structure as shown in Figure 6.

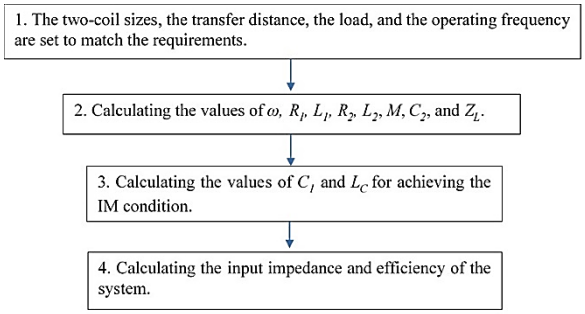

Figure 6 The design diagram

4. Design and experiment

From Figure 4, we design the proposed structure as follows: d = 5 cm, $a_1 = a_2$ = 9 cm, $b_1 = b_2$ = 0.5 mm, $p_1 = p_2$ = 1.1 mm, $h_1 = h_2$ = 12 mm, and $N_1 = N_2$ = 10 turns. The RF source is 10 V with the inner impedance Z_s = 50 Ω. The frequency operation is set to 15 kHz because the efficient RF source is available. The commonly electrical loads are an inductive load, so we assume the load to be Z_L = 15 Ω + 100 μH. Then, electrical parameters of the system are calculated by (1)-(12) and then shown in Table 1.

Table 1 Design electrical parameters

Parameter	Value	Parameter	Value
$L_1 = L_2$ (μH)	39.461	C_2 (μF)	2.8529
$R_1 = R_2$ (Ω)	0.1380	Z_s (Ω)	50
M (μH)	9.0489	Z_L (Ω)	15 + j9.4248

All the parameters in Table 1 are used to calculate L_C from (13) and C_1 from (14). As a result, L_C and C_1 are 26.132 μH and 1.6280 μF, respectively. Next, the input impedance is calculated from (19) that the value is equal to 50.00 Ω, so the system achieves the IM condition. After, the efficiency under the IM condition is calculated as 71.2701 % from (21).

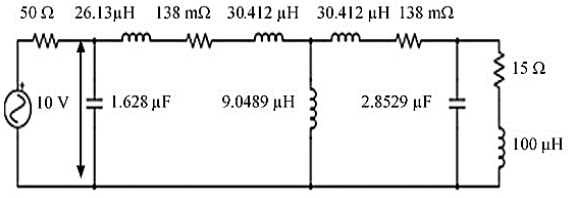

Figure 7 The equivalent circuit of this design

An Experiment is set up according to the circuit of Figure 7 which can be illustrated in Figure 8 to demonstrate the proposed concept and compared with the calculation result.

The measurement results of the input current and the load voltage are shown in Figure 9 and Table 2.

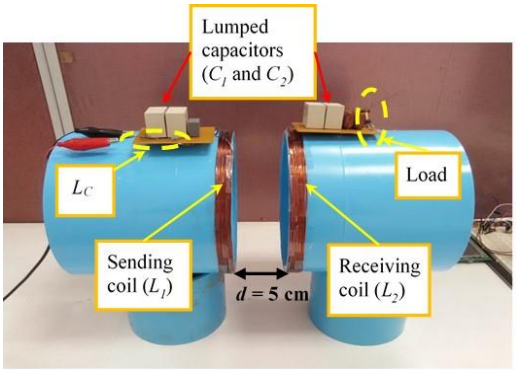

Figure 8 Experiment setup of Figure 7, the efficiency is equal to 68 %

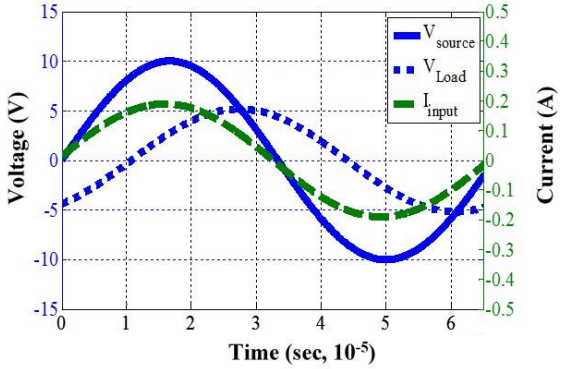

Figure 9 The measured I_{in} and V_L in the experiment

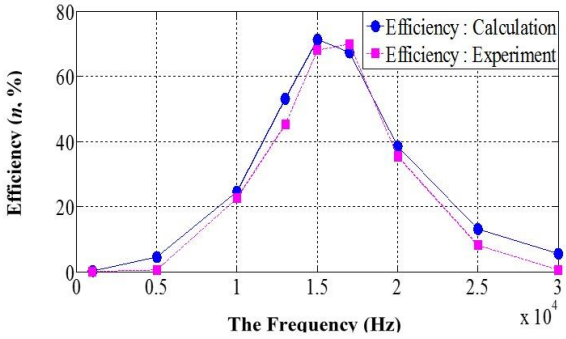

Figure 10 The efficiency versus the frequency varies

Table 2 The signals and the efficiencies

V_s = 10 V	$V_s/Z_{in} = I_{in}$ (A)	V_L (V)	η (%)
Calculation	0.2∠0°	5.46∠-53.26°	71.27
Experiment	0.19∠4°	5.19∠-57.8°	68

Figure 10 shows the IM condition at the low frequency of 15 kHz with the transfer distance of 5 cm, and the highest efficiency in the experiment is the IM condition at the operating frequency of 17 kHz.

From the experiment, the input current is measured as 0.19∠4° A as a result of the input impedance that value approximates 52.63∠-4° Ω, so the system of the experiment can proceed close to the IM condition. Furthermore, the system is conducted by varying the transfer distance from 1 to 9 cm in a step of 1 cm at setting the parameters as

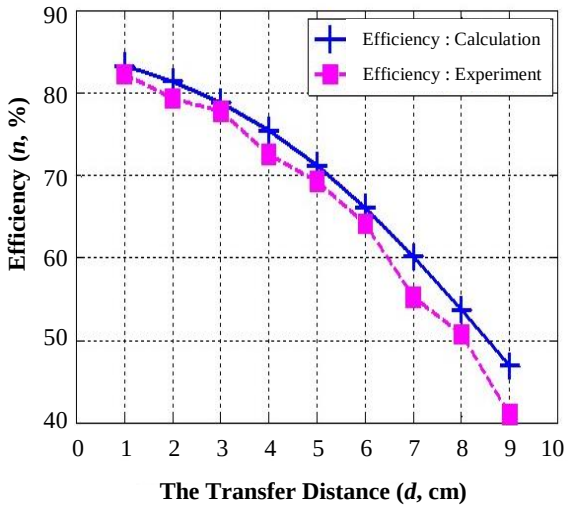

Figure 11 The efficiency versus the distance variation

presented above, while also maintaining the IM condition. The efficiencies of the calculations and the experiments can be shown in Figure 11.

From Figure 11, the efficiency of the system is continuously reduced due to lower the mutual inductance.

5. Conclusion

The papers in WPT field have usually presented the SR and strong coupling structures at operating the high frequency of greater than 1 MHz for obtaining the high efficiency, and they operate at an optimal parameter and a resistive load for achieving the IM condition. But the high frequency RF sources are usually inefficient, an optimal parameter (particular value) limits the design, and the common loads are complex.

This paper presents the modified two-coil PR structure that can operate at a low frequency for obtaining the high efficiency, and the IM condition can be achieved at a complex load and without an optimal parameter.

6. Acknowledgements

The authors would like to thank the Quantum based Engineering and Signal Processing Research Group, Faculty of Engineering, Thammasat University, for technical supports.

7. References

[1] Rittiplang A, Pijitrojana W. A Low frequency wireless power transfer using parallel resonance under impedance matching. Appl Mech Mater. 2015;781:410-3.

[2] Hui SYR, Zhong, Lee CK. A critical review of recent progress in mid-range wireless power transfer. IEEE Trans Power Electron. 2014;29(9):4500-11.

[3] Zhang Y, Zhao Z, Chen K. Frequency decrease analysis of resonant wireless power transfer. IEEE Trans Power Electron. 2014;29(3):1058-63.

[4] Zhang Y, Lu T, Zhao Z, Chen K, He F, Yuan L. Wireless Power transfer to multiple loads over various distances using relay resonators. IEEE Microw Wireless Compon Lett. 2015;25(5):337-9.

[5] Zhang Y, Zhao Z, Chen K. Frequency-splitting analysis of four-coil resonant wireless power transfer. IEEE Trans Ind Appl. 2014;50(4):2436-45.

[6] Thomas EM, Heebl JD, Pfeiffer C, Grbic A. A power link study of wireless non-radiative power transfer systems using resonant shielded loops. IEEE Trans Circ Syst. 2012;59(9):2125-36.

[7] Bodrov A, Sul Seung-Ki. Analysis of wireless power transfer by Coupled Mode Theory (CMT) and practical considerations to increase power transfer efficiency. In: Ki Young Kim, editor. Wireless Power Transfer - Principles and Engineering Explorations. Croatia: Intech; 2012. p. 19-50.

[8] Chopra S. Contactless power transfer for electric vehicle charging application [Master of Science Thesis]. Delft: Delft University of Technology; 2011.

[9] Pozar DM. Microwave engineering. 4th ed. Hoboken: John Wiley and Sons, Inc.; 2005.